Effect of a gelatinous media in concrete setting: I. Changes in Surface Morphology Model

Edgardo J. Suárez-Dominguez[1]*, Eduardo Arvizu-Sánchez[1], Josue F. Pérez-Sánchez[1], Elena F. Izquierdo-Kulich[2]

[1] *FADU-Universidad Autónoma de Tamaulipas, Centro Universitario Sur-89000. Tampico, Tamaulipas. México.*

[2] *Departamento de Química-Física, Domicilio conocido. Universidad de la Habana. La Habana, Cuba.*

Abstract : *Concrete is the most widely used materials for its strength and durability, as well as its manageability. However, it is generally related to the high levels of emissions it produces. It is possible to find additives that improve the setting properties of concrete and increase its mechanical resistance to compression. However, It is necessary to elucidate the specific reason for this. In the present work, a stochastic model was developed to predict changes in the surface area for solids obtained by mixing with cement. Also, three gelatinous media were evaluated. (prickly pear mucilage, agar-agar and gelatin) dosed with mixtures of cement and water. It was found that the surfaces of the combinations that have gelatinous media presented lower porosity and that the compressive strength of the mixtures was higher than that designed. It implies that gelatinous medium, regardless of its chemical nature, modifies the crystallisation process on physical changes in the medium, helping to efficiently set the concrete independent of the chemical nature of the gelling product used..*

Keywords — *Composite materials, gelatinous medium, natural additives, mucilage and agar, compressive strength.*

I. INTRODUCTION

The nopal is a plant that occurs naturally in Mexico. It has properties that modify the mixtures with cement [1]. The dosage has also been carried out in lime mixtures modifying crystallisation [2]. An increase in the durability and resistance to some components has been visualised [3,4] and can be related to the formal modifications that other materials and deformation can undergo [5].

Prickly pear and organic fiber allow cement-sand mortar cost reduction [6-8]. Dosage of nopal mucilage modifies the viscosity of the mixtures and the humidity that can be obtained [9]. One of the advantages of mucilage is that it is useful even for the use of securing concrete with recycled aggregates [10,11] which can provide sustainability [12].

Dosage of mucilage modifies mechanical resistance, and capillary water absorption [13, 14] and the surface of these solids are characterised by irregularities causing the Actual area of the solid to be higher than a flat surface.

Substantial surface roughness depends on the formation processes [2]. Cement-gravel-sand mixture forms house construction materials, where homogeneity depends on the porosity and the size of aggregates, as well as on the composition of the mix [15]. Porosity increase causes a higher specific surface area, as well as permeability, which leads to deterioration of the solid and, ultimately, of the house.

A stochastic model with fractal geometry is proposed to estimate the behaviour of the fractal dimension and the specific surface area corresponding to each of the types of entities that make up the dispersed phase. The proposed model was used to estimate the effect of three products on surface morphology to determine if they are appropriate to reduce surface roughness and porosity.

II. METHOD

At the laboratory level, concrete mixtures were produced separately, with nopal mucilage solution, agar-agar solution and gelatin solution.

The nopal solution was obtained from food-grade nopal mucilage extract, food-grade Agar-Agar and gelatin, each one was prepared separately in solution with water at 70 ° C, with 0.05% by weight concentration. Mixes were carried out separately in a volume ratio of 0.289: 0.523: 0.77 cement: sand: gravel, uniformly mixed with a mechanical stirrer for 5 minutes, using each solution separately.

Compressive strength specimens were prepared following [16], mechanical compressive strength from [17] and [18] for the determination of the flexural strength using a simple beam with load in the centre of the gap.

The images with 40X magnification were obtained, with a Zeigen microscope, of the surfaces of solids obtained through a mixture indicated with the different products in order to analyse if the presence of these products influences the morphology of the surface and the estimated surface area of the solid. For the analysis of the images, the ImageJ program was used . The porosity study was carried out by analysing the micrographs, converting the original 8-bit picture of the surface to a binary image, and determining the average area (pixel) of the pores.

Considering that solids formed by a mixture of cement and sand can be visualised as dispersed three-phase systems, with two dispersed phases: solids (sand or gravel) and gas bubbles (pores) in a stable dispersion medium (cement), we developed a stochastic-fractal model..

A. Model for determining the surface area by morphological analysis

Due to the intrinsically random nature of the roughness, it is impossible to accurately determine the actual surface area, both experimentally and theoretically, where the estimated value depends on the magnification level at which the surface is observed, as well as on the method selected for measurement.
Fractal geometry describes the morphology of natural, but very complex objects, as well as irregular objects, through a parameter, called the fractal dimension, which is related to the object's ability to cover a dimensional Euclidean space. This parameter is determined from a binary image using the box-counting method, converting the image into a binary one, and dividing this image into N cells of size l, then counting the number of cells n_0 within. The procedure repeats progressively decreasing the size l, such that the fractal dimension is determined as: $f = \lim_{l\to 0} \frac{\ln n_0}{\ln N} = -\lim_{l\to 0} \frac{\ln n_0}{\ln l}$
For solid surfaces, this method is applied using an image processing program usinf pixels intensity in two perpendicular directions, assuming that the strength of the pixels is proportional to the height of the surface. The two irregular lines obtained in this way are then determined the fractal dimension. The fractal area of the S surface may be estimated by applying the fractional differential calculus such that [19, 20]:

$$S_F = k^{1-f_y} D_y^{f_y} k^{1-f_x} D_x^{f_x}(1) = \frac{k^{2-(f_x+f_y)}}{\Gamma(1+f_x)\Gamma(1+f_y)} X^{f_x} Y^{f_y} \quad (1)$$

Being X and Y the Euclidean distances between two points located on the surface in the x and y directions, respectively, D_t^n the fractional integral of order n concerning the integration variable t, f_x and f_y are the fractal dimensions of the lines irregular observed on the surface in the x and y directions, respectively, the parameter k is related to the precision of the measurement and the level of magnification of the image, among other factors and $\Gamma(t)$ is the gamma function defined as:

$$\Gamma(t) = \int_0^\infty e^{-x} x^{t-1} dx \quad (2)$$

the specific fractal area $a_{s,f}$ is defined as the quotient between the fractal area and the area corresponding to the equivalent Euclidean Surface [21], such that if $X = Y = L$, $L/k = h_{max}/h_{min}$ is considered you get :

$$a_{s,f} = \frac{S_F}{A} = \frac{1}{\Gamma(1+f_x)\Gamma(1+f_y)} \left(\frac{h_{max}}{h_{min}}\right)^{f-2} \frac{m^2}{m^2} \quad (3)$$

where h_{max} and h_{min} represent the maximum and minimum value of the height of the surface and f the fractal dimension of the surface estimated as:

$$f = f_x + f_y \quad (4)$$

specific fractal area quantifies to what extent the actual surface area increases due to the presence of roughness for area A an equivalent flat Surface [21, 22], such that the relationship can estimate the fractal area $S_F = a_{s,f} \times A\, m^2$

The specific surface area depends on the composition where solid porosity, characterised by the size of the pores and their fraction on the surface, is a reflection of the behaviour of the dispersed gas phase.

To theoretically analyse how the porosity and the size of the dispersed particles influence the fractal dimension, a mathematical model was obtained based on stochastic formalism and the foundations of fractal geometry.

Consideration for model development.

1. Two types of entities on the microscopic scale: solid (sand or gravel particles) and gas bubbles, in such a way that the variable that describes the behaviour of the system is the vector $\mathbf{n} = \begin{bmatrix} n_1 \\ n_2 \end{bmatrix}$, where n_1 is the total number of gas bubbles and n_2 is the total number of sand particles.
2. The intensive variable considered is the fractal surface area corresponding to each of the dispersed phases, in such a way that a vector defines it $\boldsymbol{\theta} = \begin{bmatrix} \theta_1 \\ \theta_2 \end{bmatrix}$;
3. The proposed criterion is that the relationship between the microscopic variable and the intensive variable is:

$$\begin{bmatrix} \theta_1 \\ \theta_2 \end{bmatrix} = \frac{1}{A}\begin{bmatrix} \gamma_1 & 0 \\ 0 & \gamma_2 \end{bmatrix}\begin{bmatrix} n_1 \\ n_2 \end{bmatrix} = \begin{bmatrix} \frac{\gamma_1 n_1}{A} \\ \frac{\gamma_2 n_2}{A} \end{bmatrix} \tag{5}$$

Where γ m^2/m^3 represents the specific surface area of each of the two types of entities that define each of the two dispersed phases, which can be estimated as $\gamma_1 = \frac{1}{d_1^2}$; $\gamma_2 = \frac{1}{d_2^2}$ where d_1 and d_2 are the diameter of the pores and of the sand particles, respectively..

4. For the fourth criterion is considered that during the Surface process formation it is assumed that the following methods occur, with their corresponding transition probabilities *W* per unit time: *i*) Increasing in 1 of n_1: $W_{n_1+1,n_2} = \Phi_1$; *ii*) Increasing in 1 of n_2: $W_{n_1,n_2+1} = \Phi_2$; *iii*) decreasing in 1 from n_1: $W_{n_1-1,n_2} = k_1 n_1$; and *iv*) reducing in 1 from n_2: $W_{n_1,n_2-1} = k_2 n_2$. From the established considerations, the Fokker-Planck equation is obtained, which describes the behaviour of the probability that the value of the surface area of is equal to θ at time t:

$$\begin{aligned} \frac{\partial P(\boldsymbol{\theta};t)}{\partial t} &= -\frac{\partial}{\partial \theta_1}(\gamma_1\phi_1 - k_1\theta_1)P(\boldsymbol{\theta};t) - \frac{\partial}{\partial \theta_1}(\gamma_2\phi_2 - k_2\theta_2)P(\boldsymbol{\theta};t) \\ &+ \frac{1}{2}\frac{\gamma_1}{A}\frac{\partial^2}{\partial \theta_1^2}(\gamma_1\phi_1 + k_1\theta_1)P(\boldsymbol{\theta};t) + \frac{1}{2}\frac{\gamma_2}{A}\frac{\partial^2}{\partial \theta_2^2}(\gamma_2\phi_2 + k_2\theta_2)P(\boldsymbol{\theta};t) \end{aligned} \tag{6}$$

Where $\phi_1 = \frac{\Phi_1}{A}$: $\phi_2 = \frac{\Phi_2}{A}$

Equation (6) is linear in the sense of transition probabilities per unit of time so that in steady-state, the probability function is normal or Gaussian with expected value and variance defined as:

$$\begin{aligned} &\theta_1 = \gamma_1\frac{\varphi_1}{k_1}; \quad \theta_2 = \gamma_2\frac{\varphi_2}{k_2} \\ &\sigma_1 = \frac{\gamma_1}{2A}\left(\theta_1 + \frac{\gamma_1\varphi_1}{k_1}\right); \quad \sigma_2 = \frac{\gamma_2}{2A}\left(\theta_2 + \frac{\gamma_2\varphi_2}{k_2}\right); \quad \sigma_{12} = 0 \end{aligned} \tag{7}$$

where the magnitude Λ f the internal fluctuations is determined through the determinant associated with the covariance matrix σ [23, 24]:

$$\Lambda = \frac{1}{A^2}\frac{\gamma_1\gamma_2}{4}\left(\theta_1 + \frac{\gamma_1\phi_1}{k_1}\right)\left(\theta_2 + \frac{\gamma_2\phi_2}{k_2}\right) \tag{8}$$

the hypothesis is that the fractal dimension D_f is related to the stochastic character of the excess surface. In a steady-state, it can be assumed in this case the ergodicity property, which implies equality between the temporal and ensemble averages. This consideration establishes that the temporal behaviour of a site on the surface is equivalent to the average observed at several sites simultaneously, so the fraction of sites at which a certain value of the specific surface area can be estimated from the value expected probability:

$$\rho = P_{\theta=b} = \frac{N_{\theta=b}}{N_t} = \int [P(\boldsymbol{\theta})]P(\boldsymbol{\theta})d\boldsymbol{\theta} \tag{9}$$

Although there are methods as [25] and [26], if the determinant of the matrix of the variances and covariances is expressed as a function of powers of $\theta_1 = \varepsilon_1^2$ y $\theta_2 = \varepsilon_2^2$, respectively, and the concept of fractal geometry,

the following expression is obtained to estimate the fractal dimension based on the relative composition of the dispersed phases::

$$D_f = 4 - \frac{1}{1+\gamma_1\beta_1} - \frac{1}{1+\gamma_2\beta_2} \tag{10}$$

where:

$$\beta_1 = \frac{\phi_1}{k_1}; \beta_2 = \frac{\phi_2}{k_2}$$

β_1 y β_2 re determined experimentally, where the obtained values depend on the composition of the solid, which in turn determines the total number of pores and sand particles present on the surface. Therefore, these parameters are related to each other in such a way that:

$$\beta_1 + \beta_2 \approx B = cte \tag{11}$$

considering $\gamma_j\beta_j << 1$ fractal dimension can be estimated approximately as:

$$D_f = 3\gamma_1\beta_1 + 3\gamma_2\beta_2 + 4\gamma_1\beta_1\gamma_2\beta_2 + 2 \tag{12}$$

Figure 1 shows the predicted fractal dimension as a function of the concentration with a smaller surface area, considering a system in which the specific surface area of the pores is equal to 2 times the specific surface area of the sand particles and the value of B associated with the composition of the system is assumed to be equal to 1. As can be seen, the fractal dimension decreases with increasing concentration of the entities with the smallest specific surface area, while it increases with the value of the specific surface area. According to this model, the inclusion of sand particles must cause a decrease in the porosity of the system and in its fractal dimension.

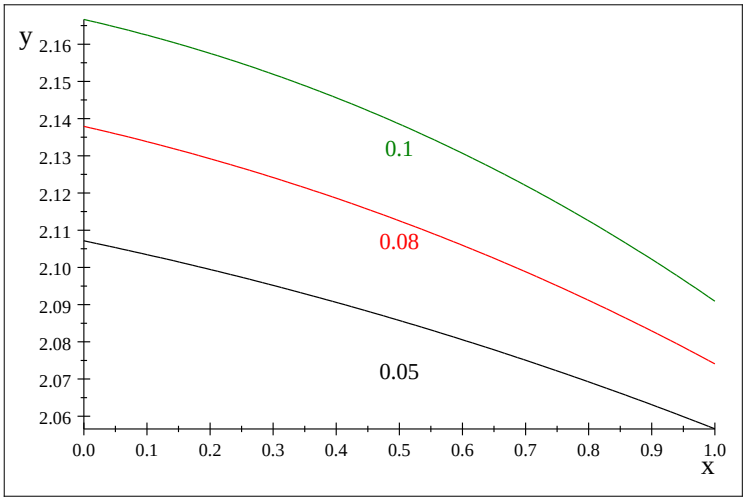

x ■ γ_2; y ■ D_f; γ_1 □ γ_2 ■ 1; $\frac{\gamma_1}{\gamma_2}$ ■ 2

Figure 1. Behaviour of the predicted fractal dimension concerning the concentration (x-axis) and particles specific surface área from equation 12.

IV. RESULTS AND DISCUSSION

Figure 2 shows the behavior of the correlation between the fractal dimension and the maximum relative height of the surface H, quantified through the quotient:

$$H = \frac{h\max}{h\min} \tag{13}$$

The maximum and minimum values of surface height depend on the depth of the pores and the diameter of the particles that make up the mixture. At the same time, the fractal dimension expresses how the particles and pores affect the morphology of the surface.

For 40X magnification is found a correlation between variables, indicating that the fractal dimension is determined by the size and distribution of voids in the solid medium.

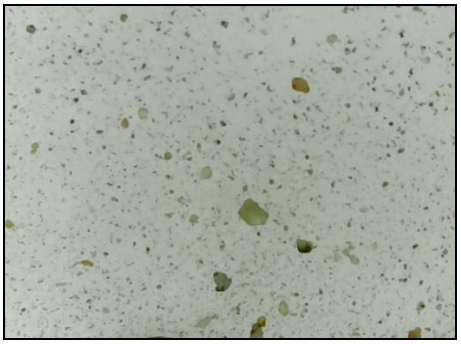

Original image

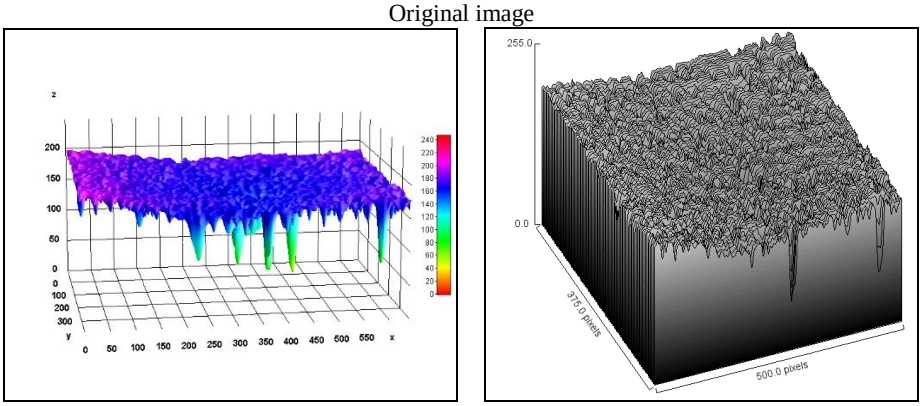

Fig. 2. Solid surface Morphology composed with gelatin a. 40X magnification picture b. 3D reconstruction indicating height scales and c. Reconstruction through irregular lines.

Figure 2. Solid surface Morphology composed with gelatin a. 40X magnification picture b. 3D reconstruction indicating height scales and c. Reconstruction through irregular lines.

Figures 3 a and 3 b show the fractal dimension values and the estimated specific fractal area for the considered magnification levels. The amount of the average diameter of the dispersed phase is .

a.

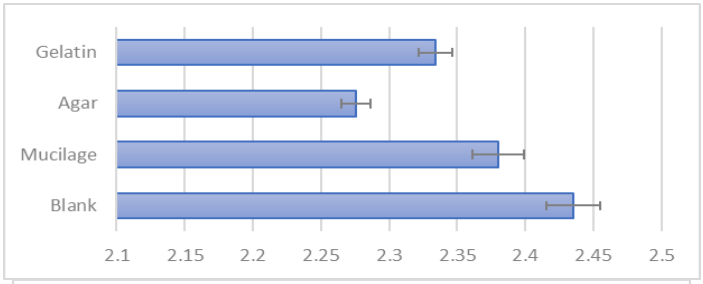

b.

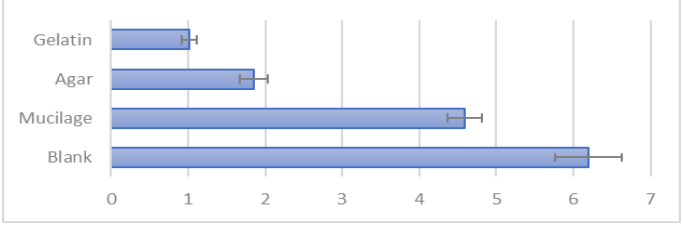

Fig. 3. Influence of the products in a concrete surface: a. on the fractal dimension and b. the estimated specific fractal área.

In the morphological study carried out, it was found that the presence of the gelatinous products in the aqueous medium modify the porosity, that is, the empty spaces available.

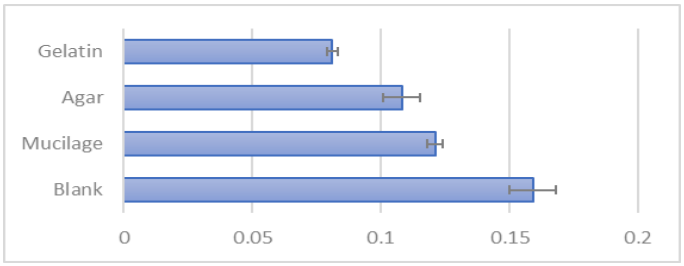

Figure 4 . The specific surface area of the pores (pixel -1) and the total number of pores per unit area in each of the samples analysed

Figure 4 shows that presence of natural products caused an appreciable decrease in the number of pores, which constitutes a result that seems to be related to a modification of the crystalline development that has been visualised in other works such as [2] that occur during surface formation, thus reducing porosity. The presence of natural products not only change the number of pores but also affect the size of these. In this case, it is observed that with respect to the target, the surface area reduces by 25%, 70% and 83% and the pore area by 23%, 32% and 49% for dosages of mucilage, agar and gelatin, respectively.

When comparing the predicted results in Figure 1 with the observed experimental results, we have a correlation coefficient of 0.9801.

The mechanical resistance to compression test was carried out, finding that the sample without dosing any product obtained a value of 17,652, 20,595, 19,711 and 20.04 for the blank, mucilage, agar and gelatin, respectively, with a maximum error of 2%. For the results of the flexion test, no significant differences were found between the values of the mixtures.

One of the primary contributions of this work is that dosage of natural products not only promote steric stabilisation that limits aggregation of crystals, improves the colloidal nature of the mixtures, but also increases the capacity of keeping water in the pores improving setting, regardless of the chemical nature of the three products, which modifies the physical growth of the crystals thermodynamically. This is also compatible with mortars as obtained in [27] and other mixes with cement.

V. CONCLUSION

From the stochastic formalism based on the master equation and the foundations of fractal geometry, we obtained a model to predict the fractal surface area of a multiphase system made up of three components, a solid that forms the dispersion medium, a second solid that is the aggregate that is dispersed within the former and dispersed gas, responsible for the presence of surface porosity. The model was applied to study the effect of three components on the specific surface area of the surface of a solid consisting mainly of a concrete mixture , where the components treated were gelatin, agar and mucilage , reducing the surface area by at least 25% .

From the observed experimental results and the use of the model, it was shown that the dosage of prickly pear mucilage, agar-agar or gelatin, significantly reduces the fractal surface area and increases the mechanical resistance to compression.

REFERENCES

[1] Carrillo, C. H., Gómez-Cuaspud, J. A., & Suarez, C. M. (2017, December). Compositional, thermal and microstructural characterisation of the Nopal (Opuntia ficus indica), for addition in commercial cement mixtures. In *Journal of Physics: Conference Series* (Vol. 935, No. 1, p. 012045). IOP Publishing.

[2] Rodriguez-Navarro, C., Ruiz-Agudo, E., Burgos-Cara, A., Elert, K., & Hansen, E. F. (2017). Crystallisation and colloidal stabilisation of Ca (OH) 2 in the presence of nopal juice (*Opuntia ficus indica*): implications in architectural heritage conservation. *Langmuir*, *33*(41), 10936-10950.

[3] Torres-Acosta, A. A., & Díaz-Cruz, L. A. (2020). Concrete durability enhancement from nopal (opuntia ficus-indica) additions. *Construction and Building Materials*, *243*, 118170.

[4] Hernández, E. F., Cano-Barrita, P. D. J., & Torres-Acosta, A. A. (2016). Influence of cactus mucilage and marine brown algae extract on the compressive strength and durability of concrete. *Materiales de Construcción*, *66*(321), 074.

[5] Jianming, Y., Luming, W., & Jie, Z. (2019). Experimental study on the deformation characteristics of magnesium potassium phosphate cement paste at early hydration ages. *Cement and Concrete Composites*, *103*, 175-182.

[6] El Azizi, C., Hammi, H., Chaouch, M. A., Majdoub, H., & Mnif, A. (2019). Use of Tunisian Opuntia ficus-indica Cladodes as a Low Cost Renewable Admixture in Cement Mortar Preparations. *Chemistry Africa*, *2*(1), 135-142.

[7] Kammoun, Z., & Trabelsi, A. (2019). Development of lightweight concrete using prickly pear fibres. *Construction and Building Materials*, *210*, 269-277.

[8] Blanco, Y. D., Campos, E. C. M., Valdés, C. I. R., & Chavarín, J. U. (2019). Natural additive (nopal mucilage) on the electrochemical properties of concrete reinforcing steel. *Revista ALCONPAT*, *9*(3), 260-276.

[9] León-Martínez, F. M., Cano-Barrita, P. D. J., Lagunez-Rivera, L., & Medina-Torres, L. (2014). Study of nopal mucilage and marine brown algae extract as viscosity-enhancing admixtures for cement-based materials. *Construction and Building Materials*, *53*, 190-202.
[10] Gunasekar, S., Ramesh, N., & Shivani, G. (2019). Effective Utilisation of Construction and Demolition Waste (Cdw) As Recycled Aggregate in Concrete Construction–A Critical Review. *International Research Journal of Multidisciplinary Technovation*, *1*(6), 465-469.
[11] McNeil, K., & Kang, T. H. K. (2013). Recycled concrete aggregates: A review. *International Journal of Concrete Structures and Materials*, *7*(1), 61-69.
[12] Behera, M., Bhattacharyya, S. K., Minocha, A. K., Deoliya, R., & Maiti, S. (2014). Recycled aggregate from C&D waste & its use in concrete–A breakthrough towards sustainability in construction sector: A review. *Construction and building materials*, *68*, 501-516.
[13] Binici, H., & Aksogan, O. (2018). Durability of concrete made with natural granular granite, silica sand and powders of waste marble and basalt as fine aggregate. *Journal of Building Engineering*, *19*, 109-121.
[14] Tosun, Y., & Şahin, R. (2015). Compressive Strength and Capillary Water Absorption of Concrete Containing Recycled Aggregate. World Academy of Science, Engineering and Technology, International Journal of Civil, Environmental, Structural, Construction and Architectural Engineering, 9(8), 987-991
[15] Hettiarachchi, C., & Mampearachchi, W. K. (2020). Effect of surface texture, size ratio and large particle volume fraction on packing density of binary spherical mixtures. Granular Matter, 22(1), 8.
[16] NMX-C-251-1997-ONNCCE Industria de la Construcción – Concreto – Elaboración y Curado de Especímenes de Ensayo.
[17] NMX-C-083-ONNCCE-2014. Norma Mexicana, Determinación de la resistencia a la compresión de especímenes. (2014).
[18] NMX-C-303-ONNCCE-2010. Norma Mexicana, Determinación de la resistencia a la flexión usando una viga simple con carga en el centro del claro (2010).
[19] Sabatier, J. Agrawal, O.P. Tenreiro Machado, J. A. Advances in Fractional Calculus: Theoretical Developments and Applications in Physics and Engineering. 2007 Springer
[20] Miller KS, Ross B (1993) An Introduction to the Fractional Calculus and Fractional Differential Equations. Wiley, New York
[21] Mandelbrot, B. The Fractal Geometry of Nature. W. H. Freeman, New York, 1983.
[22] Peitgen, H.O. and Saupe, D.. The Science of Fractal Images. Springer-Verlag, New York, 1986.
[23] Van Kampen, N.G. Stochastic Processes in Physics and Chemistry; Elsiever, Holand, 2007
[24] Gardiner, C. Stochastic Methods: A Handbook for the Natural and Social. Sciences (Springer, Berlin, 2009)
[25] Nitesh M Sureja, Sanjay P Patel. Solving A Combinatorial Optimization Problem Using Artificial Fish Swarm Algorithm *International Journal of Engineering Trends and Technology*, 68(5),27-32.
[26] Seydou Youssoufa, Moussa Sali, Nkongho Anyi Joeph, Abdou Njifenjou (2020). Calculation of thin, isotropic circular Plates subject to constant loading by the Generalized Equations of Finite Difference Method *International Journal of Mathematics Trends and Technology*, 163-176.
[27] Suárez-Domínguez, E. J., Aranda-Jiménez, Y. G., Fuentes-Pérez, C., & Zúñiga-Leal, C. (2017). Behavior of the heat capacity and ultrasonic characterisation for poured earth. *Journal of Mechanical and Civil Engineering*. 14[6] 18-22.